Supporting Information

Dual-Salt-Enabled Atomic Engineering of Zn-N_4 Sites through Na/Cl Modulation for High-Performance Bifunctional Oxygen Electrocatalysis

Zhixin Wang[a], Yingjie Chen[a,*], Tengyu Zhang[a], Fanzhen Kong[a], Likai Jin[a], Beili Pang[a], Qian Zhang[a], Jianguang Feng[a,*], Liyan Yu[a,*], and Lifeng Dong[a,b,*]

[a]College of Materials Science and Engineering, Qingdao University of Science and Technology, Qingdao 266042, China

[b]Department of Physics, Hamline University, St. Paul 55104, USA

[*]Corresponding authors. E-mail: donglifeng@qust.edu.cn, ldong03@hamline.edu (Lifeng Dong), liyanyu@qust.edu.cn (Liyan Yu), fengjg@qust.edu.cn (Jianguang Feng), and chenyingjie@qust.edu.cn (Yingjie Chen).

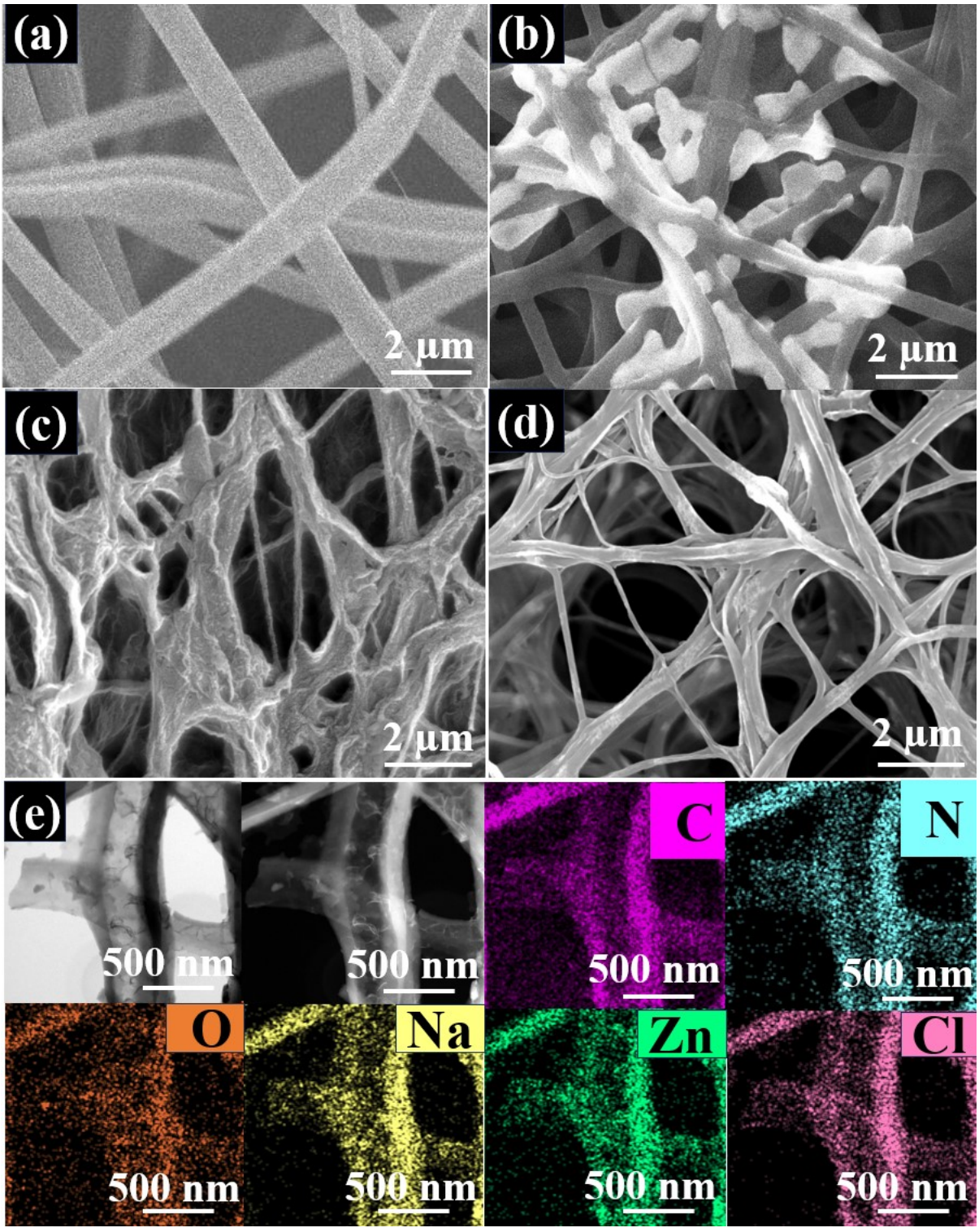

Figure S1. SEM images of (a) Na-Fs, (b) ZnNa-Fs-300, (c) ZnNa-CFs-800, and (d) ZnNa-CFs-1000. (e) TEM image of ZnNa-CFs-500 with the corresponding EDS elemental mapping results.

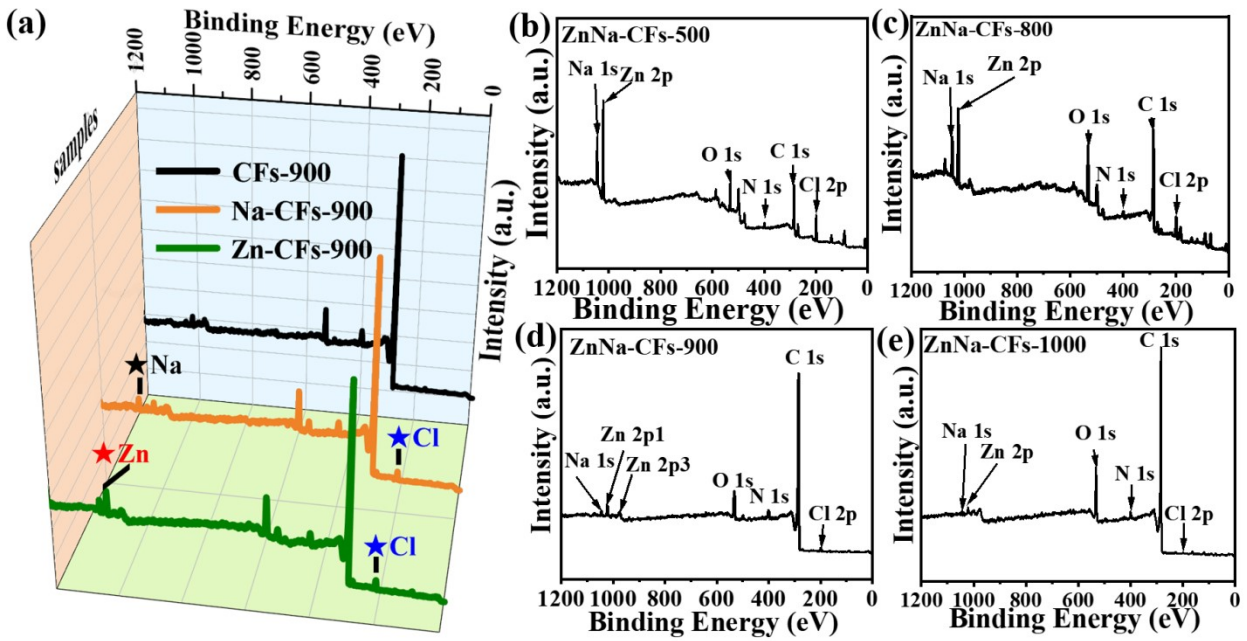

Figure S2. (a) Comparative XPS survey spectra of CFs-900, Na-CFs-900, and Zn-CFs-900 presented in a three-dimensional stacked view. XPS survey spectra of (b) ZnNa-CFs-500, (c) ZnNa-CFs-800, (d) ZnNa-CFs-900, and (e) ZnNa-CFs-1000.

Table S1. EXAFS fitting parameters at the Zn K-edge for the various samples.

Sample	Path	N	R（Å）	σ^2（10^{-3} Å^2）	E_0（eV）	R-factor
Zn Foil	Zn-Zn1	6	2.64 (0.004)	11.33 (1.38)	2.34 (1.45)	0.005
	Zn-Zn2	6	2.80 (0.02)	2.54 (5,32)		
ZnNa-CFs	Zn-N	1.29 (0.21)	2.03 (0.02)	3.16	7.04 (1.04)	0.015
	Zn-Cl	2.41 (0.17)	2.27 (0.01)	3.87		
Zn-CFs	Zn-N	2.09 (0.14)	1.97 (0.02)	4.53	4.47 (1.33)	0.011
	Zn-Cl	0.88 (0.11)	2.25 (0.01)	0.40		

[a]*CN*, coordination number; [b]*R*, distance between absorber and backscattering atoms; [c]σ^2, Debye-Waller factor accounting for thermal and structural disorders; [d]ΔE_0, inner-potential correction; The *R* factor indicates the goodness of fit. The amplitude reduction factor (S_0^2) was fixed at 0.90 based on the experimental EXAFS fitting of Zn foil with the CN constrained to its known crystallographic value. Reasonable ranges for EXAFS fitting parameters are: $0.600 < S_0^2 < 1.000$; $CN > 0$; $\sigma^2 > 0$ Å^2; $|\Delta E_0| < 15$ eV; *R* factor < 0.02.

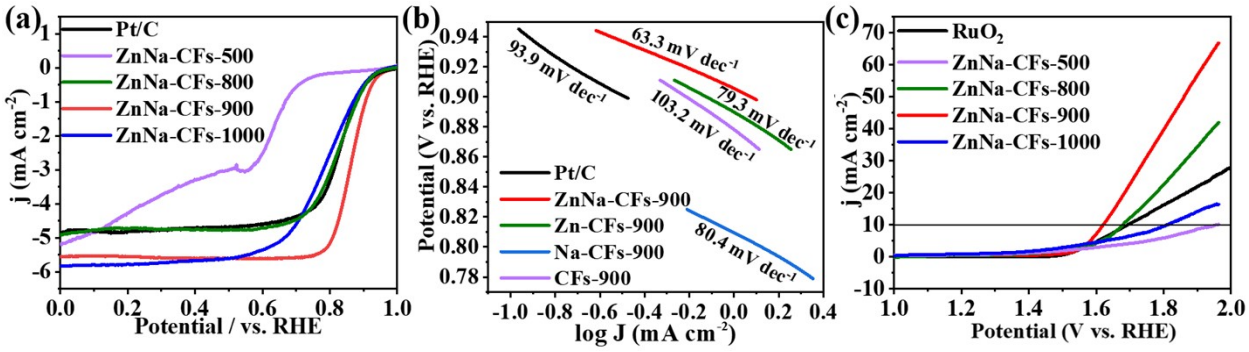

Figure S3. (a) ORR polarization curves of various CFs compared with Pt/C. (b) Tafel slopes of the CF samples for ORR. (c) OER polarization curves of various CFs compared with RuO_2.

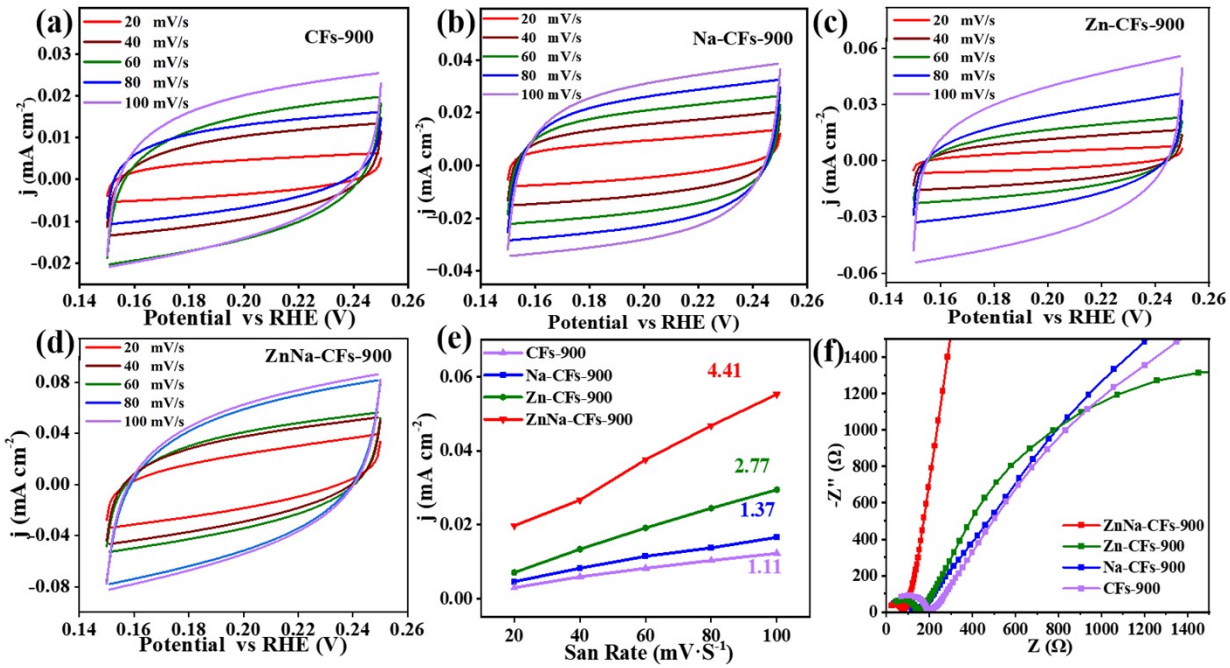

Figure S4. CV curves of (a) CFs-900, (b) Na-CFs-900, (c) Zn-CFs-900, and (d) ZnNa-CFs-900 recorded at sweep rates of 20-100 mV/s. (e) Current density versus sweep rate and (f) Nyquist plots for the four samples.

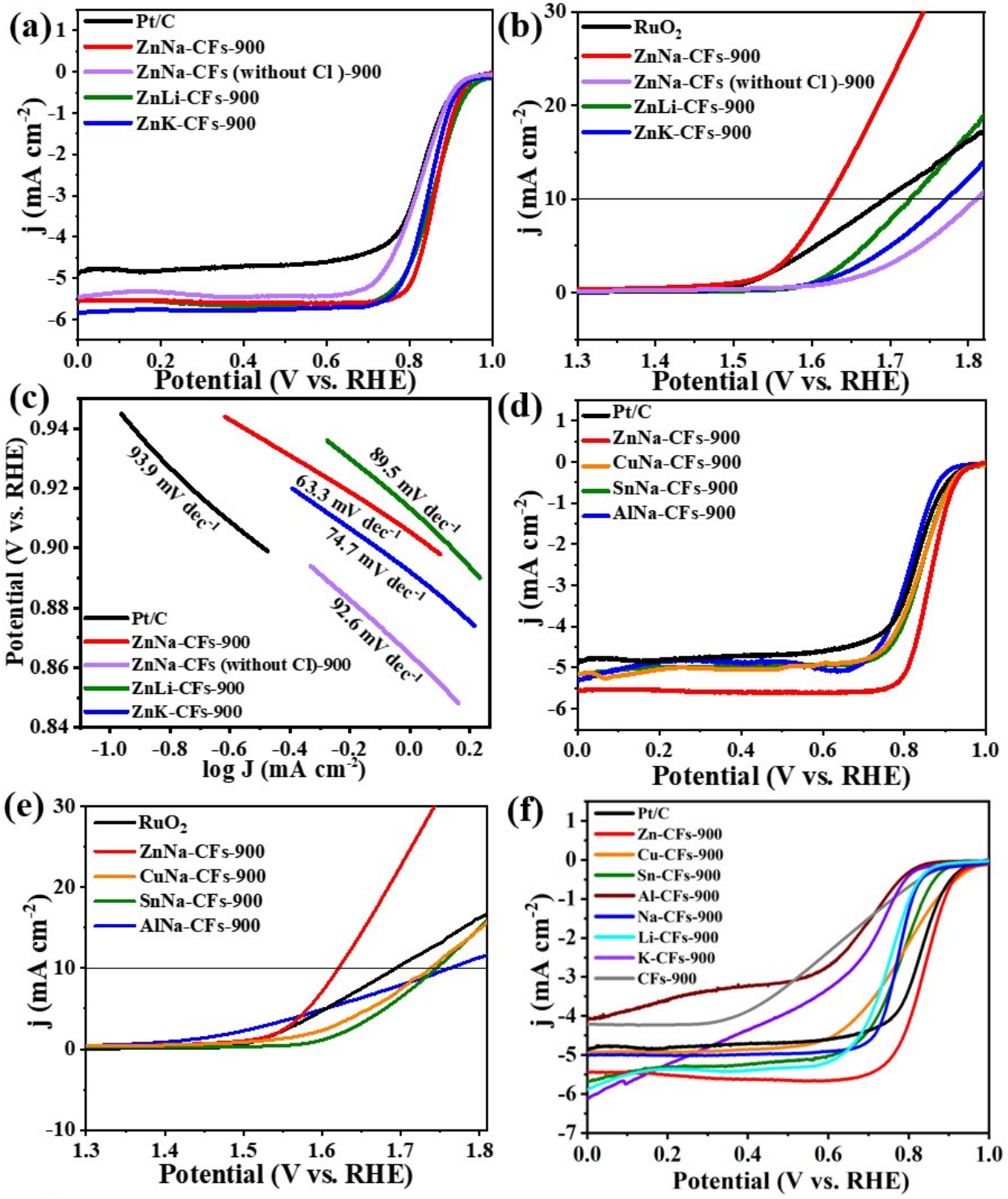

Figure S5. (a) ORR and (b) OER polarization curves of the Zn-based catalysts. (c) Tafel slopes for ORR. (d) ORR and (e) OER polarization curves of the Na-regulated catalysts. (f) ORR polarization curves.

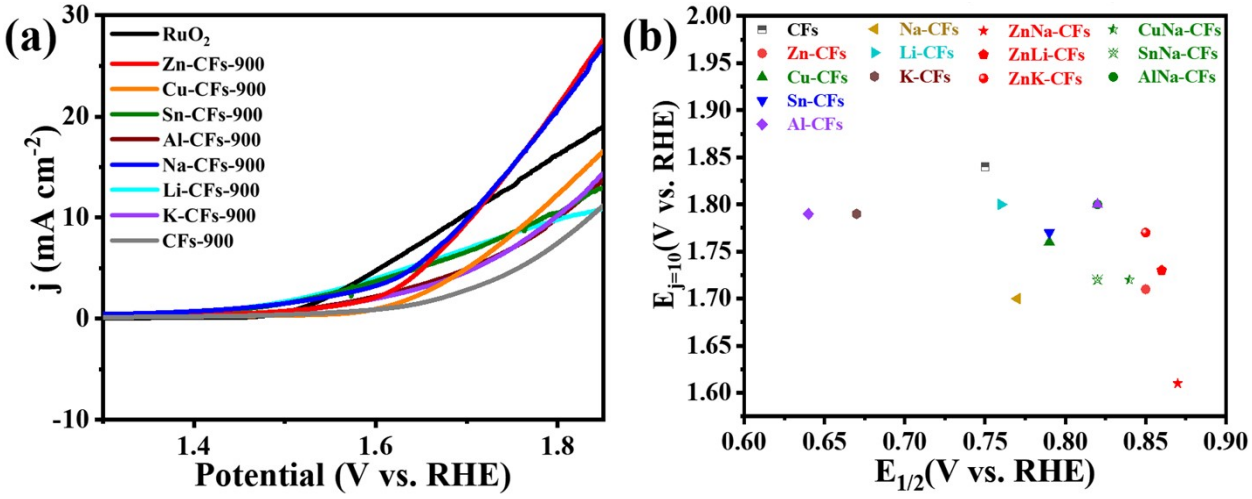

Figure S6. (a) OER polarization curves. (b) Summary plot comparing the ORR and OER activities of all samples.

Table S2. Comparison of ORR and OER activities of ZnNa-CFs-900 with other recently reported noble metal-free catalysts[1-6].

Catalysts	E_{onset} (V vs. RHE)	$E_{1/2}$ (V vs. RHE)	J_l (mA cm^{-2})	$E_{j=10}$ (V vs. RHE)	References
Co_4/Fe_1@NC	0.980	0.835	4.55	/	[1]
NZP-900	0.96	0.79	3.23	/	[2]
FeCoNi-N-rGO	0.89	0.836	5.11	1.67	[3]
Mn/Co-N-C-0.02-800	0.9	0.8	5.3	1.66	[4]
H-CoFe@NCNF	0.96	0.77	4.89	1.68	[5]
CoN-HPCNF		0.78	5.0	1.63	[6]
ZnNa-CFs-900	0.95	0.87	5.6	1.61	This work

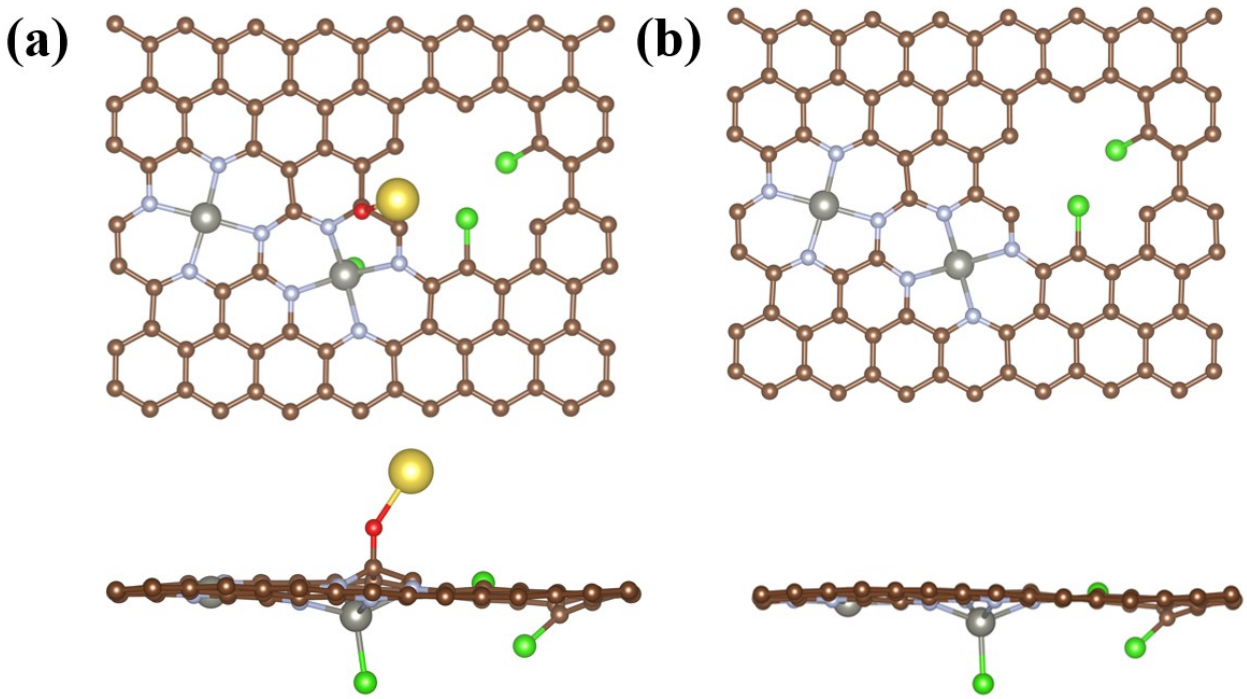

Figure S7. Molecular models of representative catalyst slabs and the corresponding adsorption configurations of oxygen intermediates (a) ZnNa-CFs, (b) Zn-CFs-900.

Table S3. Bader effective charges of two catalyst slabs

		Na	Cl(Zn-Cl)	Cl(C-Cl)-1	Cl(C-Cl)-2
Bader charge	ZnNa-CFs	-0.144	-0.741	0.004	-0.187
	Zn-CFs	/	-0.708	0.037	-0.193

References

[1] A. Han, W. Sun, X. Wan, D. Cai, X. Wang, F. Li, J. Shui, D. Wan, Construction of Co_4 atomic clusters to enable Fe-N_4 motifs with highly active and durable oxygen reduction performance, Angew. Chem. Int. Ed. 62 (2023) e202303185. https://doi.org/10.1002/anie.202303185

[2] S. Ran, J. Qi, X. Dong, H. Huang, M. Qi, W. Dong, P. Zhao, Z. Zhao, J. Yang, Molten NaCl-assisted pyrolysis of ZIF-8/PAN electrospun fibers to synthesize 1D cross-linked mesoporous N-rich carbon as oxygen reduction electrocatalysts, Chem. Eng. J. 463 (2023) 142174. https://doi.org/10.1016/j.cej.2023.142174.

[3] X. Chen, D. Chen, G. Li, C. Gong, Y. Chen, Q. Zhang, J. Sui, H. Dong, J. Yu, L. Yu, L. Dong, A hierarchical architecture of Fe/Co/Ni-doped carbon nanotubes/nanospheres grafted on graphene as advanced bifunctional electrocatalyst for Zn-air batteries, J. Alloys Compd. 873 (2021) 159833. https://doi.org/10.1016/j.jallcom.2021.159833.

[4] L. Wei, L. Qiu, Y. Liu, J. Zhang, D. Yuan, L. Wang, Mn-doped Co-N-C dodecahedron as a bifunctional electrocatalyst for highly efficient Zn-air batteries, ACS Sustain. Chem. Eng. 7 (2019) 14180-14188. https://doi.org/10.1021/acssuschemeng.9b02884.

[5] X. Zhang, P. Yu, G. Xing, Y. Xie, X. Zhang, G. Zhang, F. Sun, L. Wang, Iron single atoms-assisted cobalt nitride nanoparticles to strengthen the cycle life of rechargeable Zn-air battery, Small 18 (2022) 2205228. https://doi.org/10.1002/smll.202205228.

[6] W. Peng, X. Yang, L. Mao, J. Jin, S. Yang, J. Zhang, G. Li, ZIF-67-derived Co nanoparticles anchored in N-doped hollow carbon nanofibers as bifunctional oxygen electrocatalysts, Chem. Eng. J. 407 (2021) 127157. https://doi.org/10.1016/j.cej.2020.127157.